Journal of
Water & Climate Change

IWA PUBLISHING

Journal of Water and Climate Change Vol 14 No 8, 2531 doi: 10.2166/wcc.2023.299

Discovering spatio-temporal dependencies in mangrove forest change: evidence from northwestern Asian communities

Mojtaba Forouzannia[a] and Atefeh Chamani[b,*]

[a] Environmental Science and Engineering Department, Isfahan (Khorasgan) Branch, Islamic Azad University, Isfahan, Iran
[b] Environmental Science and Engineering Department, Waste and Wastewater Research Center, Isfahan (Khorasgan) Branch, Islamic Azad University, Isfahan, Iran
*Corresponding author. E-mail: a.chamani@khuisf.ac.ir

ABSTRACT

The Iranian southern intertidal ecosystems are colonized by mangrove forests (mostly *Avicennia marina*) and presented a notable mangrove area expansion over the past decades. To discover its spatio-temporal dependencies, five mangrove forests were studied along a coastline of more than 1,200 km. Cloud-free Landsat images were processed using a temporal median filter to produce one representative Landsat image for each year from 1988 to 2020. The images were categorized into mangrove and non-mangrove classes using an object-based algorithm and visual post-classification. A consistent mangrove area expansion was observed across all regions, which regressed linearly against time with an adjusted R^2 range of 0.914–0.955 ($p < 0.01$). The expansions were also found to be highly significantly similar ($0.182 < p < 0.822$) using the *t*-test applied on the slope of region-specific regression models. Three spatial metrics of infilling, edge-expansion, and outlying were developed to investigate the spatial pattern of expansions. Results showed the dominance of the edge-expansion pattern across all regions (53–78% of the expansions), which was attributed to the better establishment of propagules near and under the canopy of parent trees. The outlying pattern (11–22%) was related to mangrove colonization along the inland creeks.

Key words: *Avicennia marina*, Iran, Landsat, spatial metrics

HIGHLIGHTS

- The Iranian southern intertidal ecosystems are colonized by mangrove forests.
- Results exhibited a spatio-temporal harmony in the expansion of mangrove forests.
- Edge-expansion was found to be the dominant type in all regions.
- Future studies should categorize these expansion patterns into landward and seaward groups.

GRAPHICAL ABSTRACT

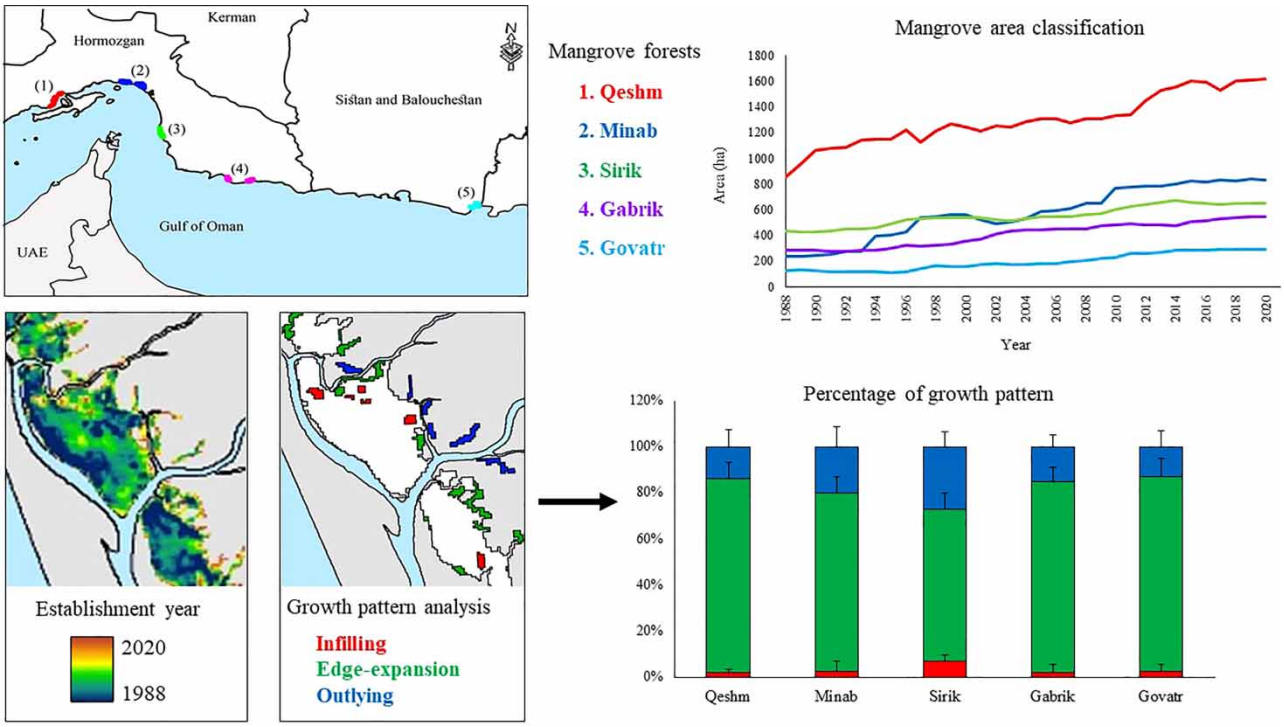

INTRODUCTION

Mangroves are a group of tropical salt-tolerant trees and shrubs that are physiologically adapted to live in extreme intertidal environments where daily tidal fluctuations expose them to variable salinity, inundation, and nutrient contents (Yan *et al.* 2017). The benefits of mangroves are manifold and mostly include shoreline protection against flood, storm, and erosion (Chow 2018), habitat provisioning for a large variety of valuable marine and terrestrial fauna, especially replenishing commercial food fish populations (Benzeev *et al.* 2017), carbon sequestration (Ahmed *et al.* 2018), and providing cultural ecosystem services (de Souza Queiroz *et al.* 2017). Despite their economic and ecological importance, mangrove forests are highly limited in distribution and vulnerable to changing climatic characteristics. Research evidence shows that mangrove forests suffer considerable degradation and area loss, probably more than any other natural environment (Hamilton 2013), due to a combination of factors such as land-use change and climate change-related hydrological alterations (Jennerjahn 2020).

A key component of mangrove forest conservation and management is to develop a holistic understanding of their responses to different interacting limiting and driving forces occurring at various spatial and temporal scales (Otero *et al.* 2019). Recent developments in satellite remote sensing and evolving classification techniques have enabled continuous monitoring of mangrove forest areas to take immediate protective actions when they begin to shrink precipitously (Wang *et al.* 2019). Landsat images have played a major role in most of the current knowledge base about mangrove forests such as area change (Suciani *et al.* 2020), mangrove disturbance mapping (de Jong *et al.* 2021), chlorophyll concentration (Omar *et al.* 2018), and early generation (Otero *et al.* 2019). Bunting *et al.* (2018) processed Landsat 5-TM and SLC-off, Landsat 8-ETM + , and some other earth observation data to release the first output of the Global Mangrove Watch initiative, identifying a global mangrove extent of 137,600 km^2 in 2010. Wang *et al.* (2018) and Mondal *et al.* (2021) found that the strengthening and weakening of some factors such as human activities and tidal range changes are the main causes of the mangrove area changes detected from multi-temporal Landsat images in southeast China.

Besides knowing the areal extent of mangrove forests, a great deal of interest has been also devoted to measuring the spatial patterns of mangrove forests (Thaxton *et al.* 2007). Mangrove forests exhibit varying spatial dispersion by species and region. The single-species (*Avicennia marina*) mangrove forests of New Zealand have grown in the seaward fringe of previously existing mangrove patches in sheltered estuaries and harbor inlets. Similarly, Long *et al.* (2021) showed that favorable suspended

sediment concentration in estuarine environments results in horizontal seaward edge-expansion of mangrove forests in the Red River Delta, Vietnam. Mondal *et al.* (2021) revealed that erosion and accretion processes can create new islands with detached and scattered mangrove patches in intertidal zones. Different patterns of mangrove area colonization and retreat were also observed by Asbridge *et al.* (2019) in the Kakadu National Park, northern Australia, which mirrored the sea level rise in the region. Despite the widespread mangrove expansion patterns of edge-expansion and outlying, interior (infilling) patterns were not reported in the existing literature due to the unique spatial dispersion of mangrove forests.

Southeastern Iran is quite underdeveloped and hosts a few local coastal human populations. Except for the Qeshm region on the northern coast of the Strait of Hormuz, other Iranian mangrove forests are inaccessible and remained intact for decades. Over the past two decades, low-energy coastal shrimp farms have been extensively developed in the supra-tidal zone of the regions hosting mangrove forests in southern Iran to take advantage of the tidal movement for water renewal (Hadipour *et al.* 2015). Moreover, changing the lifestyle of local people from energy and economic dependency on natural resources (such as mangroves) to other forms of energy and services and changing the sediment-erosion budget of the intertidal zones have allowed the mangrove forests to extend their distribution. In the present research, a coupled Remote Sensing and Geographic Information Systems (RS-GIS) procedure was employed to understand the rate of mangrove expansion. Moreover, the rate of expansion was also compared between different major intertidal mangrove-covered areas to gain insight into the similarity of the processes governing the mangrove expansion. Five distinct intertidal zones along a coastal stretch of more than 1,000 km of the Gulf of Oman and the Strait of Hormuz that experienced mangrove area expansion over the past three decades were selected as case study areas. Mangrove area layers were extracted annually using a median filter applied to the Landsat images taken from 1988 to 2020. The *t*-test analysis was performed to compare the slope of the regression models fitted to mangrove area changes over time. Moreover, three spatial indices explaining infilling, edge-expansion, and outlying growth types were used to compare the spatial pattern of mangrove area change between the regions. The results were analyzed to discover spatio-temporal dependencies in mangrove forest changes along the coastal line of the Gulf of Oman and the Strait of Hormuz. Specifically, the following steps were taken in the study:

(1) Annual extraction of mangrove areas in the main Iranian mangrove areas from 1988 to 2020,
(2) Measuring the spatial growth forms of mangrove areas during the study period, and
(3) Statistical comparison of the mangrove growth rate between the regions.

MATERIAL AND METHODS

Study area

Five mangrove forests along a coastline of more than 1,200 km were selected in the north of the Strait of Hormuz and the Gulf of Oman (Figure 1). These forests are confined to intertidal ecosystems due to arid conditions between 25° 10′ and 27° 10′ northern latitudes. From west to east, Qeshm (also known as Khamir), Minab, and Sirik are located along the northern coasts of the Strait of Hormuz. The Qeshm mangrove forest (55° 54′ E.L–26° 85′ N.L) is located at the mouth of the Mehran River reaching the Persian Gulf and is designated as the Protected Area (Zahed *et al.* 2010). The Minab mangrove forest (56° 70′ E.L–27° 10′ N.L) is composed of two spatially distinct forests of Kouleghan and Tiyab, of which only 1.3 ha of the Tiyab area is decreed as an International Wetland. The Sirik mangrove forest (57° 09′ E.L–27° 17′ N.L) is also established as International Wetland, while the Gabrik mangrove forest (58° 10′ E.L–25° 34′ N.L) is a non-protected area in the east of Jask Port. The Govatr mangrove forest (61° 57′ E.L–25° 10′ N.L) is situated in the delta of the Bahookalat River and is part of the Gandoo Protected Area (Zahed *et al.* 2010). Except for Sirik, the selected mangrove forests are composed of mono-species communities of *A. marina* (family Avicenniaceae – known as Harra). In Sirik, Harra and *Rhizophora macrunata* (family Rhizophoraceae – known as Chandal) have created a two-species mangrove forest such that Chandal trees, accounting for 21% of the region's mangrove trees, are predominantly located on the seaward edge of the mangrove patches (Askari *et al.* 2022). The mean annual rainfall in the selected mangrove forests is less than 200 mm with no permanent freshwater resources coming from the northern highlands (Zahed *et al.* 2010).

Methods

Time-series mangrove area classification

The area of mangrove forests was extracted from Landsat data. With a spatial resolution of 30 m and a revisit time of 16 days (and 8 days after the availability of Landsat 9), it provides mid-resolution images for accurate systematic vegetation mapping

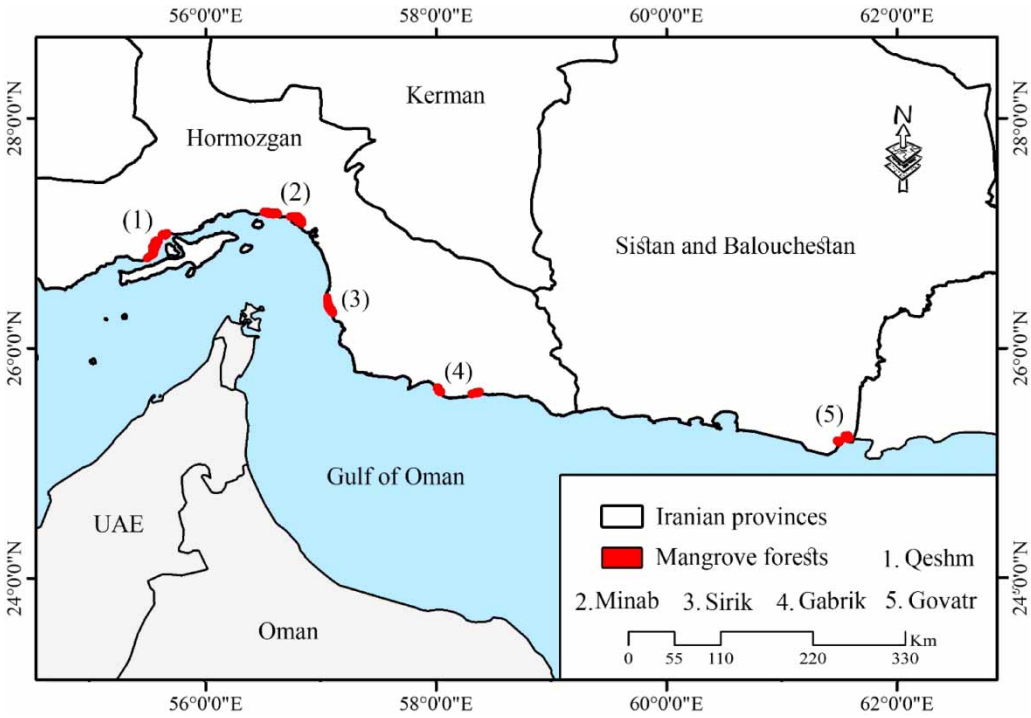

Figure 1 | Location of Qeshm, Minab, Sirik, Gabrik, and Govatr mangrove forests along the northern coasts of the Strait of Hormuz and the Gulf of Oman.

and monitoring across the world. The surface reflectance-corrected Landsat images (spatial spacing of nearly 30 m) were freely acquired from the Google Earth Engine (GEE) platform. The GEE service enables fast and accurate acquisition of RS images at many correction and processing levels ranging from raw data to combined and temporally filtered images even at the pixel level (Mutanga & Kumar 2019). The images from 1988 to 1999 and from 2008 to 2013 were obtained from Landsat 5-TM. Landsat 7-ETM+ data were used for the years 2000–2007 and Landsat 8-OLI data were used for the years from 2014 to 2020. To have one representative Landsat image for each year, the temporal median filter (Behling *et al.* 2018) was applied to all of the cloud-free images (cloud cover of less than 1%) that were present each year. This algorithm also filled the Landsat 7-ETM + scan gaps using the non-gap pixels that were available in other images of that year. The object-based classification procedure using a multi-resolution segmentation algorithm and extensive visual post-classification inspection was undertaken to categorize each image into mangrove and non-mangrove classes. The segmentation algorithm utilized a bottom-up unsupervised approach that merges nearby pixels based on local homogeneity criteria (Tian & Chen 2007). Using multiple trial-and-error runs, the scale of image segmentation (in WGS 1984 geographical coordinates), shape, and compactness in the image segmentation procedure were set to be 15, 0.5, and 0.5 for all images. The near-infrared band (band 5 in Landsat 8 and band 4 in Landsat 5 and 7) was also considered twice as important as other bands. Except for occasional surface cyanobacteria accumulations, mangrove trees, seawater, and sandy/muddy lands were the only and highly distinctive cover types in all intertidal zones and images, which enabled their accurate identification and classification.

Reference points to validate image classification were unavailable for the majority of the years. To address this challenge, around 50 reference points were selected from the edge of mangrove patches, starting from 1988. Based on field surveys and relying on the tree age estimates of a mangrove expert, if the age of the mangrove tree(s) located exactly at each reference point was older than the age of the image and the corresponding pixel was classified as mangrove, it was assumed as a correct classification in the confusion matrix. To reduce fieldwork, the same mangrove age-known reference points were used to validate every subsequent image if the mangrove patch remained relatively unchanged (both in terms of the areas and Normalized Difference Vegetation Index (NDVI) values) over the years, which reduced the number of reference points from 1,600 unique points to 384 points. One confusion matrix was created for each year and two indices of the Kappa coefficient and overall accuracy (Du *et al.* 2014) were calculated to evaluate the classification validity. Due to the small number of cover types (mangrove and non-mangrove classes) and their high spatial distractibility, it was assumed that the Kappa

coefficient and overall accuracy values of above 0.9 indicate an acceptable classification; otherwise, the classification procedure was repeated to yield the desired accuracy.

Comparison of the mangrove annual expansion

The Landsat-derived mangrove areas were compared regionally in terms of the area change rate, the maximum annual percentage of area gains and losses, and the area and year of minimum and maximum coverage from 1988 to 2020. Different types of regression analysis were then applied to each region to identify the best linear or nonlinear model explaining the annual expansion of mangrove areas over the past three decades. Given that the mangrove area change followed an increasing linear pattern in all regions, the slopes of the regression lines were compared using the two-tailed Student *t*-test to determine pairwise statistical similarity in the annual expansion of mangrove forests between the regions. We hypothesized that a *p*-value of less than 0.05 ($p < 0.05$) indicates that changes in the mangrove forest areas are governed by different or, at least, the same but temporally different driving forces.

Spatial patterns of mangrove expansion

Landscape metrics are quantitative indices that characterize various aspects of the landscape spatial pattern from a single patch to a mosaic of different land uses (del Castillo *et al.* 2015). To date, a broad collection of landscape metrics has been developed to understand the spatio-temporal changes in the composition, structure, and configuration of land surface characteristics (Hesselbarth *et al.* 2019). In this research, three metrics of infilling, edge-expansion, and outlying were utilized to characterize the annual growth of mangrove forests. These three metrics were basically developed to measure different types of urban growth using the ratio of common perimeter between previously existing and newly developed patches (Wilson *et al.* 2003). Different from static landscape metrics, these metrics represent the structural and configurational changes of land surface characteristics over time and are well suited for the temporal comparison of highly dynamic cover types. Especially, these metrics are highly capable of change detection analysis to show the dependency of newly developed areas on old patches. To measure these metrics, mangrove patches were first converted to the vector format to calculate the perimeter of all mangrove patches (L_T) and the common perimeter they have with those of the preceding year (L_C). Using Equation (1), a perimeter ratio of 0 indicates the outlying pattern, and 1 indicates the infilling pattern; otherwise, it was considered the edge-expansion pattern (see Figure 4). Finally, a comparison was made in the area and spatial patterns of mangrove loss and gain from 1988 to 2020.

$$\text{Perimeter ratio} = L_C/L_T \tag{1}$$

RESULTS

The mangrove forest areas were extracted satisfactorily with acceptable mean Kappa coefficient and overall accuracy values of more than 0.918 and 0.971. The most accurate results were obtained in Sirik where mangrove trees have created dense and compact forest patches, while the accuracy statistics were the lowest in Govatr and Minab, respectively (Table 1). All mangrove forests showed consistent and sustained expansion over the study period (Figure 2). To visually illustrate the 1988–2020 growth area of mangrove forests, a heat map was produced in Figure 3. In this figure, every pixel is labeled by the number of years hosting mangrove trees during the study period. Hence, dark blue pixels represent initial mangrove regions, while Seville orange pixels are those established in the years leading to 2020. The minimum area of mangrove forests was observed during the first 4 years of 1988–2020, while it peaked in 2014 in Sirik and in 2019–2020 in other regions (Table 1). The maximum annual growth of 23.92 ha was observed in Qeshm, so the area of its mangrove forest increased from 854.22 ha in 1988 to over 1,619.60 ha in 2020. The Govatr region had the least mangrove cover of 116.47 ha in 1991, which increased to about 294.53 ha in 2019 with a mean annual growth rate of 5.23 ha. Changes in the mangrove area were highly dynamic across all regions. A notable increase in the area of mangrove forests such as the annual growth percentages of 11.27 and 10.96 observed in Minab and Govatr, respectively, was mostly related to afforestation projects administered by governmental organizations.

The parameters of the best regression model fitted to the annual growth of mangroves are given in Table 1, indicating that mangrove area expansion is a linear function of time across all regions. All regression models were significant at $p < 0.01$ and showed an adjusted R^2 range of 0.914–0.955 (Table 2). The results of pairwise comparison between the slopes of the linear

Table 1 | Statistics of mangrove area change and accuracy assessment derived from Landsat images from 1988 to 2020

Statistics		Region				
		Qeshm	Minab	Sirik	Gabrik	Govatr
Minimum	Area (ha)	854.22	233.33	425.33	276.26	116.47
	Year	1988	1989	1990	1991	1991
Maximum	Area (ha)	1,619.61	843.60	673.89	543.56	294.53
	Year	2020	2019	2014	2020	2019
Net change (ha)		765.39	610.27	248.56	267.3	178.06
Mean annual growth (ha)		23.92	18.72	6.88	8.18	5.23
Maximum annual gain (%)		8.38	11.27	8.34	9.89	10.96
Maximum annual loss (%)		−3.52	−4.10	−1.36	−2.85	−4.86
# of reference points per year		50	50	50	50	50
Kappa coefficient	Range	0.908–0.936	0.900–0.953	0.901–0.958	0.909–0.962	0.904–0.945
	Mean	0.924	0.919	0.942	0.923	0.918
Overall accuracy	Range	0.947–0.991	0.948–0.987	0.948–0.973	0.958–0.981	0.979–0.996
	Mean	0.982	0.977	0.990	0.972	0.971

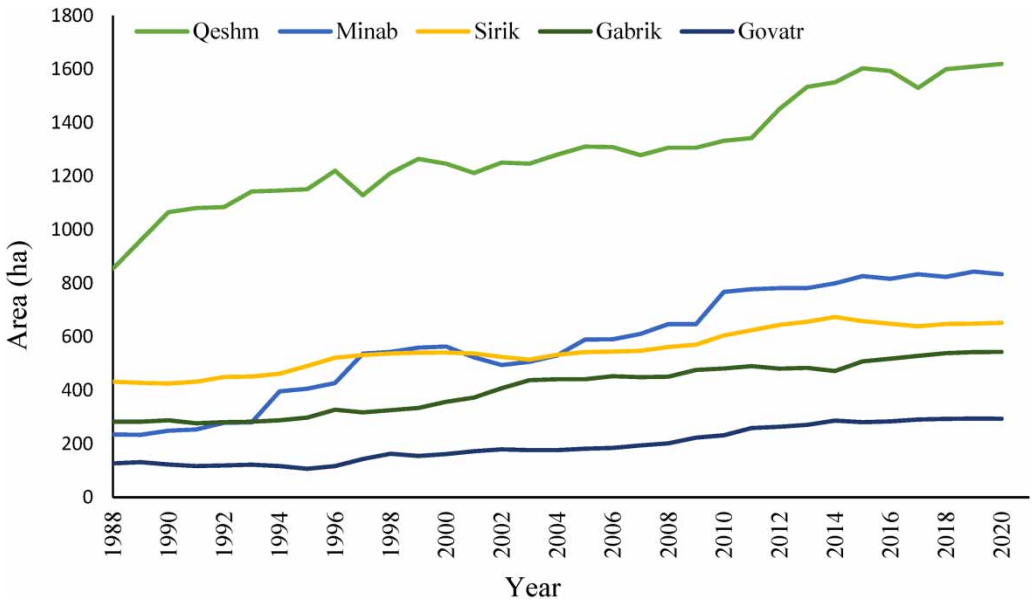

Figure 2 | Trend of mangrove area change derived from Landsat images from 1988 to 2020 in Geshm, Minab, Sirik, Gabrik, and Govatr regions.

regression models are presented in Table 3. Accordingly, none of the differences were statistically significant at the 1% level, indicating that the rate of annual change in the mangrove forest areas was similar between the regions.

A representative example of infilling, edge-expansion, and outlying growth patterns that occurred in the Sirik forest is shown in Figure 4. The regional mean percentage of mangrove growth patterns is also given in Figure 5. Edge-expansion was the dominant growth pattern in all regions, specifically in the easternmost regions of Govatr and Gabrik, which accounted for 78.04 and 74.87% of the patterns. The lowest edge-expansion growth was observed in the two-species mangrove forest of Sirik (52.85%). The infilling pattern was rare across all regions and ranged between 1.70 in Gabrik and

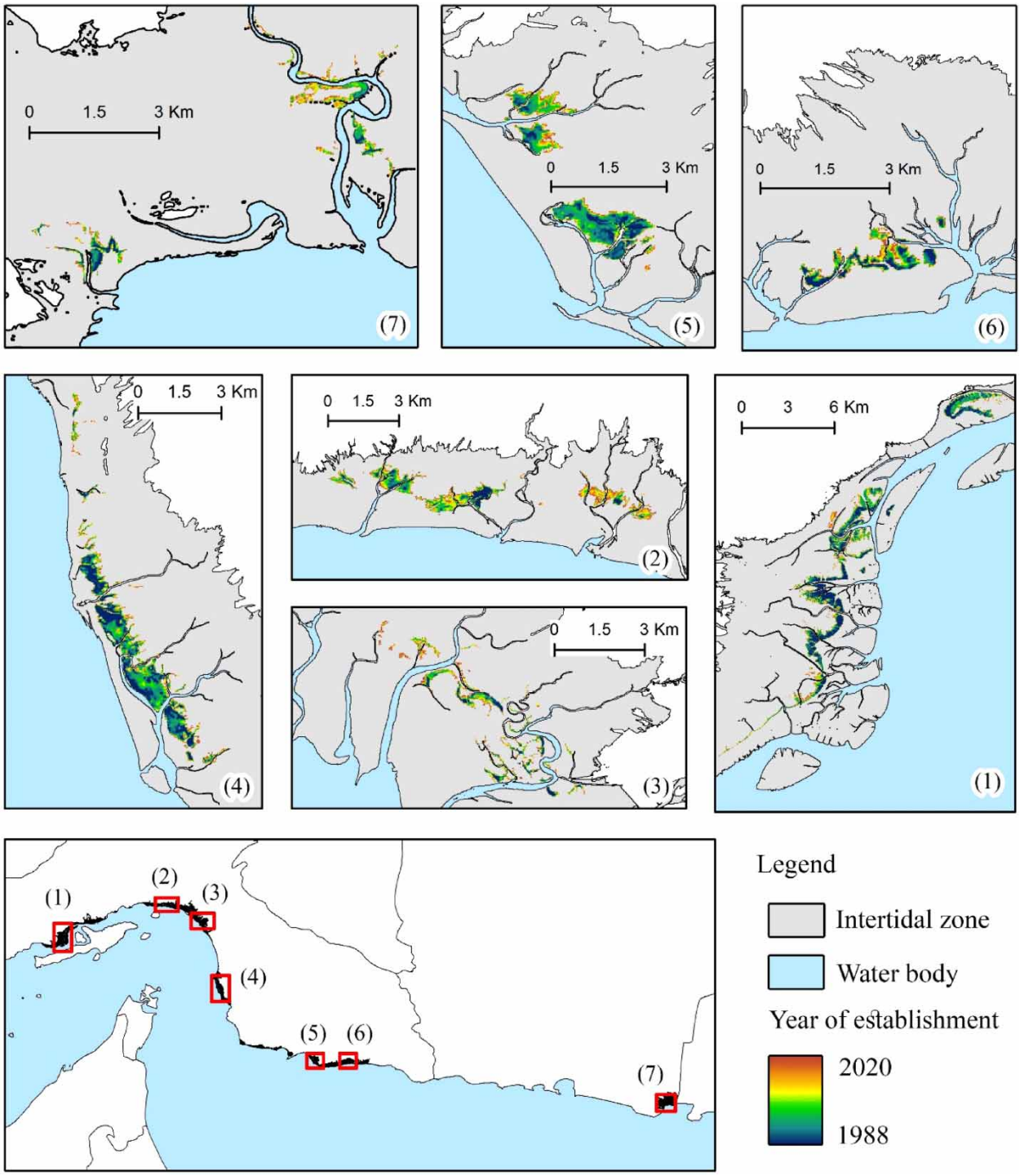

Figure 3 | Spatial distribution of the annual growth of mangrove trees derived from the classification of Landsat images from 1988 to 2020.

5.52 in Sirik. The lowest and highest area percentage of the outlying pattern was observed in Qeshm (11.17%) and Sirik (21.61%), respectively. In general, the infilling, edge-expansion, and outlying patterns accounted for 2.63, 66.94, and 14.80% of the area of mangrove expansion that occurred across all regions from 1988 to 2020. Moreover, the standard deviation of the expansion patterns was relatively low, indicating that the growth percentages were relatively constant over the study period. In other words, the annual growth of mangroves was close to their long-term mean in all regions.

Table 2 | Statistics of the best-fit regression model applied to the growth of mangrove areas from 1988 to 2020

		Coefficients		Model summary		
Region	**Model type**	**Intercept**	**Slope**	***F***	**Sig.**	**Adjusted R^2**
Qeshm	Linear	1,983.37	35.94	360.42	0.000	0.918
Minab	Linear	1,988.27	27.06	154.61	0.000	0.928
Sirik	Linear	1,988.97	29.49	330.24	0.000	0.914
Gabrik	Linear	1,990.66	27.07	664.37	0.000	0.955
Govatr	Linear	1,992.79	24.47	438.62	0.000	0.934

Table 3 | Results of *t*-test analysis conducted between the slopes of the best-fit linear regression models

	Two-tailed *t*-statistics (*p*-value)				
Region	**Qeshm**	**Minab**	**Sirik**	**Gabrik**	**Govatr**
Qeshm	–	0.619 (0.537)	0.643 (0.522)	0.357 (0.721)	1.346 (0.182)
Minab	0.619 (0.537)	–	1.094 (0.277)	0.402 (0.689)	0.225 (0.822)
Sirik	0.643 (0.522)	1.094 (0.277)	–	0.743 (0.459)	1.136 (0.259)
Gabrik	0.357 (0.721)	0.402 (0.689)	0.743 (0.459)	–	0.501 (0.617)
Govatr	1.346 (0.182)	0.225 (0.822)	1.136 (0.259)	0.501 (0.617)	–

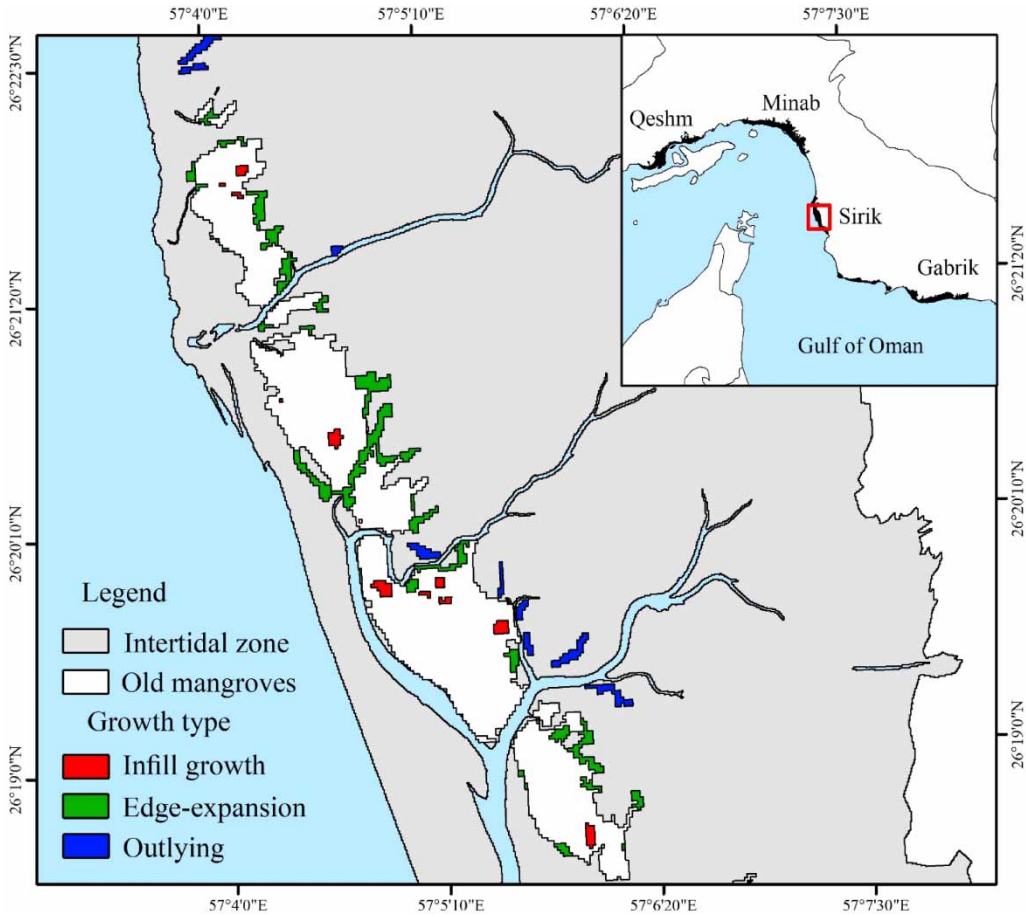

Figure 4 | Representative examples of infilling, edge-expansion, and outlying growth patterns occurring in the Sirik forest.

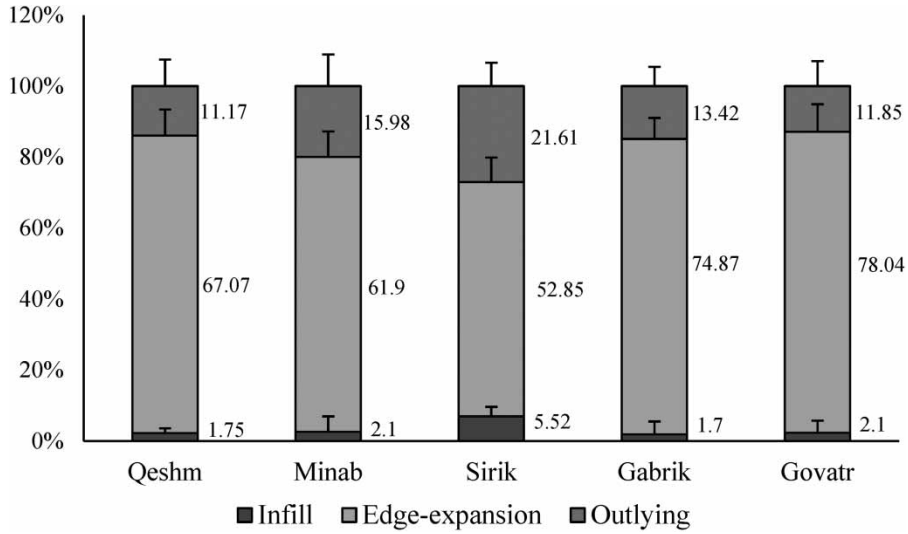

Figure 5 | Percentage of infilling, edge-expansion, and outlying growth patterns occurring in Qeshm, Minab, Sirik, Gabrik, and Govatr regions from 1988 to 2020.

DISCUSSION

Mangrove forests are highly dynamic and face frequent changes in their spatial distribution and above-ground (structure) biomass. In southern Iran, the mangrove forest cover loss is due to limited clear-cutting, unsustainable selective cuttings, and also partial canopy dieback events resulting from intensive drought stresses (Mafi & Jaafari 2020; Asgarian & Soffianian 2023). In this research, the mangrove area loss was found to be minimal, displaying no spatio-temporal uniformity across study landscapes, and was not significantly related to impacts of anthropogenic activities such as setting up of shrimp mariculture ponds and fishing ports. The increase in mangrove cover in Iran (maximum annual mangrove cover increase of 32.5 ha per year), however, compensated for such losses observed particularly in Qeshm and Minab (Zangane Asadi *et al.* 2019; Mafi & Jaafari 2020). Contrary to the global declining trend of mangrove forest areas around the world (Goldberg *et al.* 2020), our results showed that Iran's southern mangrove forests expanded considerably during 1988–2020. To some degree, this expansion could be due to the nutrient-rich return flows from widespread supra-tidal shrimp farms, which improve the land's ecological suitability for further mangrove expansion. In agreement with this conclusion, Asgarian & Soffianian (2023) revealed that the expansion of mangrove forests in the Minab region is related to increasing sediment total nitrogen and total phosphorus near supra-tidal shrimp farms, with levels sometimes reaching up to 30 and 45 mg/kg, respectively. Notable expansions such as those observed in Sirik (maximum of 8.34%) and Minab (maximum of 11.27%) regions are the outcomes of the efforts funded by the Hormozgan Agricultural and Natural Resources Research Center in the early 2000s and early 2010s (there are not reliable estimates of their area, but it seems to be less than 5 ha in each region according to field surveys), while the majority of the expansion was of the gradual but steady expansion of *A. marina* by natural propagation, which is indicative of a healthy, self-sustaining mangrove ecosystem.

Existing research shows that some mangrove species are highly adapted to estuaries. Particularly, *A. marina* is a distinguished pioneer of estuarine ecosystems and even is termed an invader in newly introduced intertidal zones (Hoppe-Speer *et al.* 2015). The area of mangrove forests regressed linearly against time in all regions from 1988 to 2020, indicating that the mangrove expansion in the study areas witnessed a steady growth rate over the study period even with periodic massive plantations. This linearity is also demonstrated by Asgarian & Soffianian (2023) in the expansion of the Minab mangrove forests. In agreement with our results (linear associations), Williams & Meehan (2004) and Hoppe-Speer *et al.* (2015) also found that the occupation of new habitats by *A. marina* occurs in a steady linear fashion through time. These steady patterns show the existence of factors whose effects are not instant and sharp but steady over time, such as the gradual accumulation of nutrients in the sediments (Asgarian & Soffianian 2023). Moreover, the *t*-test was utilized to compare the annual rate of area expansion between different regions based on the slope of the regression models fitted to all observations. Despite significant geomorphological and geographical differences between the regions,

the annual expansion of mangrove trees was found to be highly significantly similar over time, meaning that the regions experienced similar annual percentages of area gains and losses because of similarity in major driving forces. Due to significant morphological and altitudinal disparities, the similarity in the mangrove expansion trends may be related to regionally homogeneous factors such as climate change and its impacts on seawater characteristics or locally important factors such as the effect of tidal regimes or the growing expansion of similar supra-tidal shrimp farms in the landward side of all study landscapes. Shrimp farms are built in supra-tidal zones of sandy coasts and would not spatially affect the mangrove forest but provide nutrient-rich return flows that improve mangrove expansion. Moreover, considering that socioeconomic characteristics such as the development of ports and harbor facilities as well as protection practices remain constant, there might be regional driving forces whose impacts equally stimulate the growth and expansion of mangrove forests.

Mangroves such as *A. marina* have adopted a viviparous reproductive strategy in which seeds stay attached to the parent tree until pollination and germination into propagules, then drop to take root in the sediment (Hong *et al.* 2018). Depending on tidal and hydrologic characteristics in shallow waters, propagules might establish near and even under the canopy of the parent tree or be transported farther to establish new habitats. In this research, it seems that propagules were more successful near the parent trees, such that more than 50% of the expansions were edge-expansion as new fringe trees. The effect of this parameter was quantified by Asgarian & Soffianian (2023) in mangrove landscapes of Iran, showing that proximity to the existing mangrove patches defines the most suitable habitats for the natural reproduction of mangrove trees. As shown in Figure 4 and elaborated in detail by Peterson & Bell (2015), this type of expansion is more likely to occur in the landward periphery of old mangrove patches where the effect of tides and currents is not such as to impair the propagule establishment. In the Sirik region, the majority of the tidal flow energy is funneled into some wide channels penetrating deeply into the intertidal zone. Hence, the relatively higher percentage of the outlying growth pattern (21.61%) observed in Sirik might be attributed to the morphological characteristics of the region and landward propagule transportation along the main channels, which created mangrove-lined creeks (see Figure 4).

This growth pattern of mangrove forests seems to be a function of the landscape morphological characteristics, helping propagules to colonize distant habitats. In agreement with our findings, Asbridge *et al.* (2016) also showed that new mangrove (*A. marina*) colonies grow mostly along the inland creeks. The infilling expansion type was considerably minimal (less than 6%) due to pre-occupation of the best intertidal habitats. The highest percentage of the infilling expansion pattern (approximately 5.52) was observed in Sirik. In this region, unoccupied interior spaces are sufficiently exposed to tidal flooding but have a relatively higher elevation from their surrounding tree covers to receive propagules from nearby trees. Hence, they were mostly selected as suitable habitats for mangrove afforestation (especially for *R. macrunata*) over the past two decades, during which the infilling pattern was observed more frequently.

Overall, the results of this research showed a temporal harmony in the expansion of mangrove forests in southern Iran over the past three decades. The expansion also occurred mostly on the edge of old mangrove patches, which indicates significant similarities between the regional factors governing their expansion and local factors determining their spatial distribution pattern, which could potentially follow the same trend in the upcoming decades (Asgarian & Soffianian 2023). Future research in this area should be directed toward detailed determination and comparison of (1) dynamics and changes in the regions' sediment-erosion balance, (2) morphological characteristics, and (3) climatic differences in precipitation and temperature along the 25° 10′ and 27° 10′ altitude range and their effects on the seawater hydrology, tidal circulation, and sediment morphology. Moreover, a combination of these studies with a thorough understanding of the effects of shrimp farms on mangroves and their probable disturbances as recommended by Asgarian & Soffianian (2023) and Toosi *et al.* (2022) is bound to enhance the effectiveness of these studies. A wider range of landscape metrics and their classification into landward and seaward classes may better unveil the type and strength of driving and limiting factors affecting mangrove expansion in the region. Moreover, the use of high-resolution images, whose temporal resolutions and frequencies are becoming increasingly wider, can produce more accurate and comparable results.

CONCLUSION

This study utilized Landsat images and landscape metrics to delineate changes and similarities in the distribution and structural pattern of mangrove expansion that occurred on the southern coasts of Iran during the past three decades. It was the first attempt on the northern coasts of the Strait of Hormuz and the Gulf of Oman, showing that mangrove expansion followed a

similar annual trend of expansion between different regions. Moreover, three expansion metrics of infilling, edge-expansion, and outlying were borrowed from urban planning studies to assess the spatial patterns of mangrove expansions in the study regions. Edge-expansion was found to be the dominant type in all regions due to the more successful establishment of propagules near and under the canopy of parent trees. Future studies should categorize these expansion patterns into landward and seaward groups and characterize the shrimp farms' probable effects on mangroves and the regions' topographical characteristics to get a better understanding of the effect of the sedimentation-erosion balance on the expansion of mangroves on southern coasts of Iran.

AUTHORS' CONTRIBUTIONS

All authors contributed to the study's conception and design. Material preparation, data collection, and analysis were performed by M.F. The first draft of the manuscript was written by A.C. All authors read and approved the final manuscript.

FUNDING

This work was supported by Islamic Azad University, Isfahan (Khorasgan) Branch, Isfahan, Iran.

DATA AVAILABILITY STATEMENT

All relevant data are included in the paper or its Supplementary Information.

CONFLICT OF INTEREST

The authors declare there is no conflict.

REFERENCES

Ahmed, N., Thompson, S. & Glaser, M. 2018 Integrated mangrove-shrimp cultivation: potential for blue carbon sequestration. *Ambio* **47** (4), 441–452.

Asbridge, E., Lucas, R., Ticehurst, C. & Bunting, P. 2016 Mangrove response to environmental change in Australia's Gulf of Carpentaria. *Ecology and Evolution* **6** (11), 3523–3539.

Asbridge, E., Bartolo, R., Finlayson, C. M., Lucas, R. M., Rogers, K. & Woodroffe, C. D. 2019 Assessing the distribution and drivers of mangrove dieback in Kakadu National Park, northern Australia. *Estuarine, Coastal and Shelf Science* **228**, 106353.

Asgarian, A. & Soffianian, A. 2023 Past and potential future distribution of white mangroves in an arid estuarine environment: integration of Maxent and CA-Markov models. *Marine Policy* **147**, 105345.

Askari, M., Homaei, A., Kamrani, E., Zeinali, F. & Andreetta, A. 2022 Estimation of carbon pools in the biomass and soil of mangrove forests in Sirik Azini creek, Hormozgan province (Iran). *Environmental Science and Pollution Research* **29** (16), 23712–23720.

Behling, R., Milewski, R. & Chabrillat, S. 2018 Spatiotemporal shoreline dynamics of Namibian coastal lagoons derived by a dense remote sensing time series approach. *International Journal of Applied Earth Observation and Geoinformation* **68**, 262–271.

Benzeev, R., Hutchinson, N. & Friess, D. A. 2017 Quantifying fisheries ecosystem services of mangroves and tropical artificial urban shorelines. *Hydrobiologia* **803** (1), 225–237.

Bunting, P., Rosenqvist, A., Lucas, R. M., Rebelo, L.-M., Hilarides, L., Thomas, N., Hardy, A., Itoh, T., Shimada, M. & Finlayson, C. M. 2018 The global mangrove watch – a new 2010 global baseline of mangrove extent. *Remote Sensing* **10** (10), 1669.

Chow, J. 2018 Mangrove management for climate change adaptation and sustainable development in coastal zones. *Journal of Sustainable Forestry* **37** (2), 139–156.

de Jong, S. M., Shen, Y., de Vries, J., Bijnaar, G., van Maanen, B., Augustinus, P. & Verweij, P. 2021 Mapping mangrove dynamics and colonization patterns at the Suriname coast using historic satellite data and the LandTrendr algorithm. *International Journal of Applied Earth Observation and Geoinformation* **97**, 102293.

del Castillo, E. M., García-Martin, A., Aladrén, L. A. L. & de Luis, M. 2015 Evaluation of forest cover change using remote sensing techniques and landscape metrics in Moncayo Natural Park (Spain). *Applied Geography* **62**, 247–255.

de Souza Queiroz, L., Rossi, S., Calvet-Mir, L., Ruiz-Mallén, I., García-Betorz, S., Salvà-Prat, J. & de Andrade Meireles, A. J. 2017 Neglected ecosystem services: highlighting the socio-cultural perception of mangroves in decision-making processes. *Ecosystem Services* **26**, 137–145.

Du, Z., Li, W., Zhou, D., Tian, L., Ling, F., Wang, H., Gui, Y. & Sun, B. 2014 Analysis of Landsat-8 OLI imagery for land surface water mapping. *Remote Sensing Letters* **5** (7), 672–681.

Goldberg, L., Lagomasino, D., Thomas, N. & Fatoyinbo, T. 2020 Global declines in human-driven mangrove loss. *Global Change Biology* **26** (10), 5844–5855.

Hadipour, A., Vafaie, F. & Hadipour, V. 2015 Land suitability evaluation for brackish water aquaculture development in coastal area of Hormozgan, Iran. *Aquaculture International* **23** (1), 329–343.

Hamilton, S. 2013 Assessing the role of commercial aquaculture in displacing mangrove forest. *Bulletin of Marine Science* **89** (2), 585–601.
Hesselbarth, M. H., Sciaini, M., With, K. A., Wiegand, K. & Nowosad, J. 2019 landscapemetrics: an open-source R tool to calculate landscape metrics. *Ecography* **42** (10), 1648–1657.
Hong, L., Su, W., Zhang, Y., Ye, C., Shen, Y. & Li, Q. Q. 2018 Transcriptome profiling during mangrove viviparity in response to abscisic acid. *Scientific Reports* **8** (1), 1–12.
Hoppe-Speer, S. C., Adams, J. B. & Rajkaran, A. 2015 Mangrove expansion and population structure at a planted site, East London, South Africa. *Southern Forests* **77** (2), 131–139.
Jennerjahn, T. C. 2020 Relevance and magnitude of 'Blue Carbon' storage in mangrove sediments: carbon accumulation rates vs. stocks, sources vs. sinks. *Estuarine, Coastal and Shelf Science* **247**, 107027.
Long, C., Dai, Z.-j., Zhou, X., Mei, X. & Mai, C. 2021 Mapping mangrove forests in the Red River Delta, Vietnam. *Forest Ecology and Management* **483**, 118910.
Mafi, G. D. & Jaafari, A. 2020 Changes in landward and seaward extent of mangroves in the coastal areas of the Hormozgan province. *Iranian Journal of Forest and Range Protection Research* **18** (1), 1–12.
Mondal, B., Saha, A. K. & Roy, A. 2021 Spatio-temporal pattern of change in mangrove populations along the coastal West Bengal, India. *Environmental Challenges* **5**, 100306.
Mutanga, O. & Kumar, L. 2019 Google Earth Engine Applications. *Remote Sensing* **11** (5), 591.
Omar, H., Misman, M. A. & Linggok, V. 2018 Characterizing and monitoring of mangroves in Malaysia using Landsat-based spatial-spectral variability. In: *IOP Conference Series: Earth and Environmental Science*. IOP Publishing.
Otero, V., Van De Kerchove, R., Satyanarayana, B., Mohd-Lokman, H., Lucas, R. & Dahdouh-Guebas, F. 2019 An analysis of the early regeneration of mangrove forests using Landsat time series in the Matang Mangrove Forest Reserve, Peninsular Malaysia. *Remote Sensing* **11** (7), 774.
Peterson, J. M. & Bell, S. S. 2015 Saltmarsh boundary modulates dispersal of mangrove propagules: implications for mangrove migration with sea-level rise. *PLoS One* **10** (3), e0119128.
Suciani, A., Rahmadi, M. & Islami, Z. 2020 Analyzing mangrove forest area changes in coastal zone of Langsa City using landsat imagery. In: *IOP Conference Series: Earth and Environmental Science*. IOP Publishing.
Thaxton, J. M., DeWalt, S. J. & Platt, W. J. 2007 Spatial patterns of regeneration after Hurricane Andrew in two south Florida fringe mangrove forests. *Florida Scientist* **70** (2), 148–156.
Tian, J. & Chen, D. M. 2007 Optimization in multi-scale segmentation of high-resolution satellite images for artificial feature recognition. *International Journal of Remote Sensing* **28** (20), 4625–4644.
Toosi, N. B., Soffianian, A. R., Fakheran, S. & Waser, L. T. 2022 Mapping disturbance in mangrove ecosystems: incorporating landscape metrics and PCA-based spatial analysis. *Ecological Indicators* **136**, 108718.
Wang, M., Cao, W., Guan, Q., Wu, G. & Wang, F. 2018 Assessing changes of mangrove forest in a coastal region of southeast China using multi-temporal satellite images. *Estuarine, Coastal and Shelf Science* **207**, 283–292.
Wang, L., Jia, M., Yin, D. & Tian, J. 2019 A review of remote sensing for mangrove forests: 1956–2018. *Remote Sensing of Environment* **231**, 111223.
Williams, R. & Meehan, A. 2004 Focusing management needs at the sub-catchment level via assessments of change in the cover of estuarine vegetation, Port Hacking, NSW, Australia. *Wetlands Ecology and Management* **12** (5), 499–518.
Wilson, E. H., Hurd, J. D., Civco, D. L., Prisloe, M. P. & Arnold, C. 2003 Development of a geospatial model to quantify, describe and map urban growth. *Remote Sensing of Environment* **86** (3), 275–285.
Yan, Z., Sun, X., Xu, Y., Zhang, Q. & Li, X. 2017 Accumulation and tolerance of mangroves to heavy metals: a review. *Current Pollution Reports* **3** (4), 302–317.
Zahed, M. A., Rouhani, F., Mohajeri, S., Bateni, F. & Mohajeri, L. 2010 An overview of Iranian mangrove ecosystems, northern part of the Persian Gulf and Oman Sea. *Acta Ecologica Sinica* **30** (4), 240–244.
Zangane Asadi, M., Taghavi Moghadam, E. & Akbari, E. 2019 Evaluation changes and quantification mangrove forests in Khorkhouran protected area with emphasis on hydrodynamic Strait of Hormuz. *Journal of Environmental Science and Technology* **21** (6), 213–226.

First received 5 August 2022; accepted in revised form 10 July 2023. Available online 17 July 2023